

# Imaging of Parotid Gland Masses: Diagnostic Value of Magnetic Resonance Imaging in Comparison with Histopathology

## Parotis Bezi Kitlelerinin Görüntülenmesi: Histopatoloji ile Karşılaştırıldığında Manyetik Rezonans Görüntülemenin Tanısal Değeri

Utku METE<sup>a</sup>, Rifat ÖZPAR<sup>b</sup>, Özlem SARAYDAROĞLU<sup>c</sup>, Oğuz BASUT<sup>a</sup>

<sup>a</sup>Bursa Uludağ University Faculty of Medicine, Department of Otorhinolaryngology-Head and Neck Surgery, Bursa, Türkiye

<sup>b</sup>Bursa Uludağ University Faculty of Medicine, Department of Radiology, Bursa, Türkiye

<sup>c</sup>Bursa Uludağ University Faculty of Medicine, Department of Pathology, Bursa, Türkiye

**ABSTRACT Objective:** In the diagnosis of parotid gland masses, various methods are available, with magnetic resonance imaging (MRI) being the most beneficial and preferred radiological modality by otolaryngology clinicians. This study aimed to examine the MRI characteristics of parotid gland masses and correlate them with surgical histopathology to establish the diagnostic value of preoperative imaging for accurate diagnosis and treatment planning of salivary gland tumors. **Material and Methods:** A total of 161 patients diagnosed with a parotid mass at our otolaryngology department between 2013 and 2023 were examined. The diagnostic capability of MRI was determined as sensitivity, specificity, accuracy, positive predictive value, and negative predictive value. **Results:** The sensitivity, specificity, and accuracy of MRI for diagnosing parotid malignancies were 71.4%, 92%, and 87.6%, respectively. Regarding specific types of lesions, the results for pleomorphic adenoma were 83%, 87.9%, and 86.3%; for Warthin's tumor, 85.4%, 91.5%, and 89.4%; for non-classified tumors, 65.1%, 90.7%, and 83.8%; and for non-neoplastic lesions, 80%, 100%, and 98.7%, respectively. **Conclusion:** MRI is significant in diagnosing parotid masses. Its identifiable specific findings increase the sensitivity and positive predictive value for pleomorphic adenoma and Warthin's tumor. In the management of parotid gland lesions, the support of conventional MRI with other diagnostic procedures is still necessary.

**ÖZET Amaç:** Parotis bezi kitlelerinin tanısında çeşitli yöntemler mevcuttur ve manyetik rezonans görüntüleme (MRG), kulak burun boğaz klinisyenleri tarafından en faydalı ve tercih edilen radyolojik yöntemdir. Bu çalışma, parotis bezi kitlelerinin MRG özelliklerini incelemeyi ve bunları cerrahi histopatoloji ile ilişkilendirerek tükürük bezi tümörlerinin doğru tanısı ve tedavi planlamasında preoperatif görüntülemenin tanısal değerini ortaya koymayı amaçlamaktadır. **Gereç ve Yöntemler:** 2013-2023 yılları arasında kulak burun boğaz kliniğimizde parotis kitlesi tanısı almış 161 hasta incelendi. MRG'nin tanısal yeteneği, duyarlılık, özgüllük, doğruluk, pozitif prediktif değer ve negatif prediktif değer olarak belirlendi. **Bulgular:** Parotis malignitelerinin tanısında MRG'nin duyarlılığı, özgüllüğü ve doğruluğu sırasıyla %71,4, %92 ve %87,6 olarak bulunmuştur. Belirli lezyon türlerine göre pleomorfik adenom için sonuçlar %83, %87,9 ve %86,3; Warthin tümörü için %85,4, %91,5 ve %89,4; sınıflandırılmamış tümörler için %65,1, %90,7 ve %83,8; neoplastik olmayan lezyonlar için ise %80, %100 ve %98,7 olarak tespit edilmiştir. **Sonuç:** MRG, parotis kitlelerinin tanısında önemlidir. Özellikle pleomorfik adenom ve Warthin tümörü için belirgin bulguları, duyarlılığı ve pozitif prediktif değeri artırmaktadır. Ancak parotis bezi lezyonlarının yönetiminde konvansiyonel MRG'nin diğer tanısal prosedürlerle desteklenmesi hâlâ gereklidir.

**Keywords:** Magnetic resonance imaging; parotid gland; parotid neoplasms; radiology; sensitivity and specificity; surgical pathology

**Anahtar Kelimeler:** Manyetik rezonans görüntüleme; parotis bezi; parotis neoplazmları; radyoloji; duyarlılık ve özgüllük; cerrahi patoloji

**TO CITE THIS ARTICLE:**

Mete U, Özpar R, Saraydaroğlu Ö, Basut O. Imaging of Parotid Gland Masses: Diagnostic Value of Magnetic Resonance Imaging in Comparison with Histopathology. Journal of Ear Nose Throat and Head Neck Surgery, 2025;33(1):8-16.

**Correspondence:** Utku METE

Bursa Uludağ University Faculty of Medicine, Department of Otorhinolaryngology-Head and Neck Surgery, Bursa, Türkiye

**E-mail:** utkumete@uludag.edu.tr



Peer review under responsibility of Journal of Ear Nose Throat and Head Neck Surgery.

**Received:** 12 Sep 2024

**Received in revised form:** 08 Jan 2025

**Accepted:** 08 Jan 2025

**Available online:** 20 Jan 2025

1307-7384 / Journal of Ear Nose Throat and Head Neck Surgery is the official publication of the Ear Nose Throat and Head Neck Surgery Society. Production and hosting by Türkiye Klinikleri. This is an open access article under the CC BY-NC-ND license (<https://creativecommons.org/licenses/by-nc-nd/4.0/>).

A wide range of histopathological diversities, including benign and malignant forms and non-tumorous conditions, characterize salivary gland tumors.<sup>1</sup> The parotid gland, which accounts for 75-80% of salivary gland tissues, is the largest and is more likely to develop benign tumors.<sup>2</sup> However, the submandibular and minor salivary glands have a higher chance of developing malignant tumors.<sup>3</sup>

Parotid gland tumors can present as a lump in the preauricular area, expanding into the retro-mandibular and lateral parapharyngeal space.<sup>4</sup> These tumors account for approximately 3% of all head and neck tumors.<sup>5</sup> However, certain types of inflammatory conditions that mimic tumors can make it challenging to diagnose them accurately.

Accurate diagnosis of parotid gland tumors is crucial for determining suitable treatment plans and predicting the prognosis in patients with a parotid mass. With recent technological advancements, imaging techniques have become as important as interventional cytopathological procedures in the diagnostic process.<sup>6</sup>

Recently, the imaging of the parotid area has advanced significantly with three diagnostic tests: ultrasonography (US), computed tomography (CT), and magnetic resonance imaging (MRI).<sup>7</sup> US is non-invasive, fast, and cost-effective but requires a skilled practitioner. CT identifies calcifications and bone structures but requires contrast agents and exposes patients to radiation.<sup>8</sup> MRI provides comprehensive views of the parotid region with excellent tissue discrimination and reconstruction in all planes.<sup>9</sup> Both CT and MRI provide cross-sectional images of the parotid area.

This study identified the MRI characteristics of parotid gland masses and correlate them with surgical histopathology to establish the diagnostic value of preoperative imaging.

## MATERIAL AND METHODS

### ETHICAL APPROVAL

This study was approved by the Clinical Research Ethics Committee of the Faculty of Medicine at the University Hospital with the reference number 2024-

10/18 (date: June 26, 2024). Informed consent forms were obtained from all participants after they were provided with information about the content and purpose of the study. The study was conducted in accordance with the principles of the Declaration of Helsinki.

### STUDY DESIGN AND PATIENT SELECTION

This study examined patients diagnosed with a parotid mass who underwent surgery at our otolaryngology department between January 2013 and December 2023. A total of 346 cases were treated during this period, and we conducted a retrospective investigation of these cases. The study included patients of all age groups who underwent superficial and total parotidectomy and underwent MRI scans at our institute. However, patients with recurrent parotid neoplasms requiring revision surgery, local tumors invading the parotid, or metastases to the parotid from distant sites were excluded from the study. Thus, the medical records of 161 patients were examined.

### COLLECTION AND CATEGORIZATION OF DATA AND EVALUATION OF THE MRI IMAGES

Demographic information, such as age and gender, was collected. The preoperative MRI images were obtained from the picture archiving and communication system imaging data system. An expert radiologist with 10 years of experience retrospectively evaluated T1-weighted (T1W), T2-weighted (T2W), and contrast-enhanced fat-suppressed T1W axial images. Based on the study by Christie et al., lesions that appeared hyperintense on T2W images, with smooth contours and homogeneous enhancement, were considered indicative of pleomorphic adenoma (PA).<sup>10</sup> Lesions in T2W images that had a multilocular cystic appearance without a significant contrast-enhancing solid component and marked enhancement were preliminarily diagnosed as Warthin's tumor. Lesions showing T2W hypointensity, significant contrast uptake, and irregular borders were categorized under other tumoral lesions of the parotid gland. Lesions that did not meet these criteria were placed into the preliminary non-neoplastic parotid lesion category. The otolaryngology surgeon then compared these

evaluations with the post-parotidectomy permanent histopathological results to determine the diagnostic metrics of the test, including sensitivity, specificity, accuracy, and positive and negative predictive values.

## STATISTICAL ANALYSIS

The suitability of the data for normal distribution was assessed using the Shapiro-Wilk test. For descriptive statistics, numeric data that displayed a normal distribution were presented using mean and standard deviation, while categorical data were expressed in frequency and percentage. The efficacy of the diagnostic test was determined by statistics such as sensitivity, specificity, accuracy, positive predictive value (PPV), and negative predictive value, which were calculated using the McNemar test. Statistical analyses were conducted using the IBM SPSS 28.0 software package (IBM Corp., 2021, Version 28.0, Armonk, NY: IBM Corp.), and the reliability of the results was tested at a significance level of  $\alpha=0.05$ .

## RESULTS

### DEMOGRAPHIC ANALYSIS AND HISTOPATHOLOGICAL RESULTS OF THE STUDY GROUP

Our study examined 161 patients, of which 90 were males (56%) and 71 were females (44%). The average age of the patients was  $51\pm 14.8$  years. Upon

histopathological examination, we found that 126 patients (78.3%) had benign histopathology, while 35 patients (21.7%) had malignant tumors. Among the benign group, 55 cases were diagnosed with Warthin's tumor, and 53 patients had PA. In the malignant group, we found 9 cases of ductal carcinoma and 8 patients of mucoepidermoid carcinoma. [Table 1](#) summarizes the histopathological results.

### DIAGNOSTIC VALUE OF CONVENTIONAL MRI IN PAROTIDE GLAND MASSES

Among 126 histopathologically benign cases, MRI diagnosed 116 as true negative and sensitivity was 71.4%, while from 35 malignant tumors, MRI found 25 as true positive and specificity was 92%. Thus, 141 cases were diagnosed as accurate among the study group, and the overall accuracy was 87.6%. There were 10 false positive and 10 false negative results for MRI.

Then, we detailed our evaluations to determine the value of MRI in achieving histopathological results for specific diagnoses such as PA and Warthin's tumor, whereas non-classified tumors (NCT) and non-neoplastic lesions (NNL).

### PA

There were 44 true positive cases, 95 true negative cases, 13 false positive cases, and nine false negative cases identified. The sensitivity of MRI for PAs was determined to be 83%, specificity 87.9%, accuracy

**TABLE 1:** The histopathological results of parotidectomy cases in the study group.

| Diagnosis benign                          | Number (n) | Percentage (%) | Diagnosis malignant      | Number (n) | Percentage (%) |
|---|------------|----------------|--------------------------|------------|----------------|
| Warthin's tumor                           | 55         | 43.6           | Salivary duct carcinoma  | 9          | 25.7           |
| Pleomorphic adenoma                       | 53         | 42.0           | Mucoepidermoid carcinoma | 8          | 22.8           |
| Chronic sialadenitis + sialolithiasis     | 6          | 4.7            | Acinic cell carcinoma    | 6          | 17.2           |
| Oncocytoma                                | 3          | 2.4            | Adenocarcinoma           | 4          | 11.3           |
| Benign cystic lesion                      | 3          | 2.4            | Adenoid cystic carcinoma | 2          | 5.7            |
| Myoepithelioma                            | 2          | 1.6            | Lymphoma                 | 2          | 5.7            |
| Cavernous lymphangioma                    | 1          | 0.8            | High-grade carcinoma     | 1          | 2.9            |
| Basal cell adenoma                        | 1          | 0.8            | Myoepithelial carcinoma  | 1          | 2.9            |
| Multiple phleboliths + organized thrombus | 1          | 0.8            | Angiosarcoma             | 1          | 2.9            |
| Intercalated duct adenoma                 | 1          | 0.8            | Leiomyosarcoma           | 1          | 2.9            |
| Total                                     | 126        | 100            | Total                    | 35         | 100            |

**TABLE 2:** Correlation between MRI & histopathology and diagnostic values of MRI in PA.

| MRI            | PA         | Others      | Total      |
|----------------|------------|-------------|------------|
| PA             | 44         | 13          | 57         |
| Others         | 9          | 95          | 104        |
| Total          | 53         | 108         | 161        |
| Quantity       | Number (n) | Quantity    | Percentage |
| True positive  | 44         | Sensitivity | 83.0       |
| True negative  | 95         | Specificity | 87.9       |
| False positive | 13         | Accuracy    | 86.3       |
| False negative | 9          |             |            |

MRI: Magnetic resonance imaging; PA: Pleomorphic adenoma.

**TABLE 4:** Correlation between MRI & histopathology and diagnostic values of MRI in NCT.

| MRI            | NCT        | Others      | Total      |
|----------------|------------|-------------|------------|
| NCT            | 28         | 11          | 39         |
| Others         | 15         | 107         | 122        |
| Total          | 43         | 118         | 161        |
| Quantity       | Number (n) | Quantity    | Percentage |
| True positive  | 28         | Sensitivity | 65.1       |
| True negative  | 107        | Specificity | 90.7       |
| False positive | 11         | Accuracy    | 83.8       |
| False negative | 15         |             |            |

MRI: Magnetic resonance imaging; NCT Non-classified tumor.

86.3%, PPV 77.2%, and negative predictive value 91.3% (Table 2).

### CYSTADENOMA LYMHOMATOSUM/WARTHIN'S TUMOR

The analysis found 47 true positive cases, 97 true negative cases, nine false positive cases, and eight false negative cases for cystadenoma lymphomatousum (CAL). The sensitivity, specificity, and accuracy of MRI for detecting Warthin's tumor were 85.4%, 91.5%, and 89.4%, respectively. A PPV of 83.9% and a negative predictive value of 92.4% (Table 3).

### NON-CLASSIFIED TUMOR

When evaluating MRI to detect NCT, there were 28 true-positive cases, 107 true-negative cases, 11 false-positive cases, and 15 false-negative cases. The sen-

**TABLE 3:** Correlation between MRI & histopathology and diagnostic values of MRI in CAL.

| MRI            | CAL        | Others      | Total      |
|----------------|------------|-------------|------------|
| CAL            | 47         | 9           | 56         |
| Others         | 8          | 97          | 105        |
| Total          | 55         | 106         | 161        |
| Quantity       | Number (n) | Quantity    | Percentage |
| True positive  | 47         | Sensitivity | 85.4       |
| True negative  | 97         | Specificity | 91.5       |
| False positive | 9          | Accuracy    | 89.4       |
| False negative | 8          |             |            |

MRI: Magnetic resonance imaging; CAL: Cystadenoma lymphomatousum.

**TABLE 5:** Correlation between MRI & histopathology and diagnostic values of MRI in NNL.

| MRI            | NCT        | Others      | Total      |
|----------------|------------|-------------|------------|
| NNL            | 8          | -           | 8          |
| Others         | 2          | 151         | 153        |
| Total          | 19         | 151         | 161        |
| Quantity       | Number (n) | Quantity    | Percentage |
| True positive  | 8          | Sensitivity | 80         |
| True negative  | 151        | Specificity | 100        |
| False positive | -          | Accuracy    | 98.7       |
| False negative | 2          |             |            |

MRI: Magnetic resonance imaging; NNL: Non-neoplastic lesion.

sitivity of MRI for NCT was determined to be 65.1%, specificity 90.7%, accuracy 83.8%, PPV 71.8%, and negative predictive value 87.7% (Table 4).

### NNL

The investigation of the ability of MRI to detect NNLs revealed eight true positive cases, 151 true negative cases, and two false negative cases. There were no false-positive cases for NNL. Regarding NNLs, MRI was found to have a sensitivity, specificity, and accuracy of 80%, 100%, and 98.7%, respectively. The positive predictive and negative predictive values were 100% and 98.7% (Table 5).

Figure 1 summarizes the diagnostic parameters of conventional MRI, including sensitivity, specificity, accuracy, and positive and negative predictive values for PA, CAL, NCT, NNL, and malignancies.

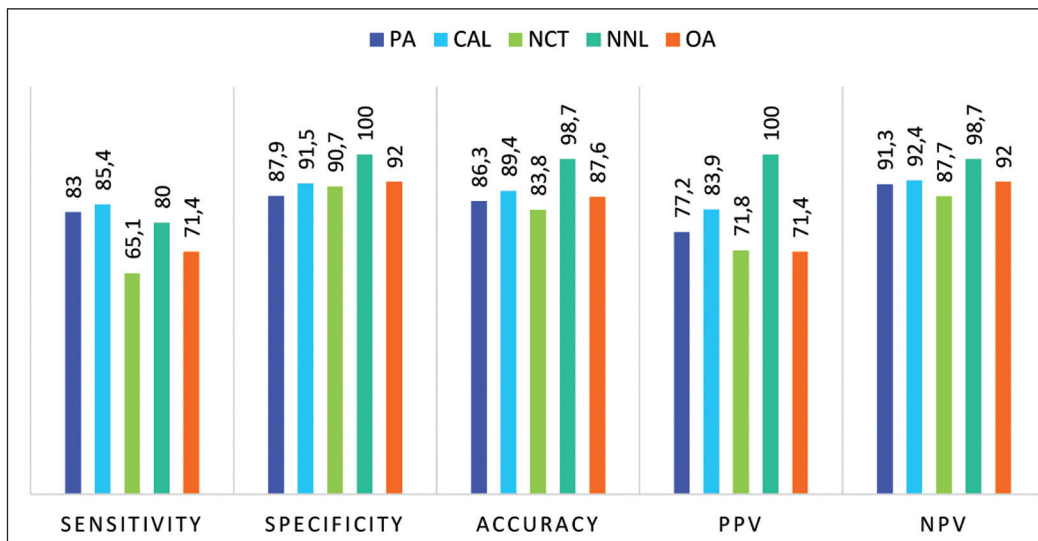


**FIGURE 1:** Diagnostic parameters of magnetic resonance imaging on evaluating different types of parotid gland masses.

PA: Pleomorphic adenoma (navy blue); CAL: Cystadenoma lymphomatosum (light blue); NCT: Non-classified tumor (lime green); NNL: Non-neoplastic lesion (mint green); OA: Overall (orange); PPV: Positive predictive value; NPV: Negative predictive value.

## DISCUSSION

In current practice, it is generally accepted to use fine needle aspiration cytology (FNAC) and MRI together for the preoperative diagnostic evaluation of masses in the parotid region.<sup>11</sup> A study conducted by Paris et al. demonstrated that for detecting malignant tumors of the parotid gland, FNAC and MRI had a sensitivity, specificity, and accuracy of 81%, 95%, and 92% and 87%, 94%, and 93%, respectively. However, using FNAC and MRI together resulted in 100% sensitivity, 88% specificity, and 91% accuracy.<sup>12</sup>

MRI is preferred over CT for examining parotid masses because it provides non-invasive cross-sectional imaging and superior soft tissue resolution.<sup>13,14</sup> Although conventional MRI scans take a long time and can be uncomfortable due to the enclosed space, new technologies are being developed to address these issues.<sup>15</sup>

Ultrasound is a fast and convenient imaging option that is safe, non-invasive, and comfortable for patients. However, it has certain limitations, such as being dependent on the operator and unable to image deeper structures. Regarding the detection of

parotid tumors, the accuracy levels of sensitivity, specificity, and accuracy are 62%, 91%, and 85%, respectively.<sup>16</sup>

The efficacy of 18-fluorodeoxyglucose positron emission tomography is currently under investigation. This assessment does not yield sufficient data for identifying parotid tumors, even when integrated with CT imaging.<sup>7</sup>

The normal parotid gland tissue is typically hyperintense compared with the surrounding muscles but hypointense compared with the fat tissue on T1W images. The gland capsule is thin and regular. The Stensen's duct runs through the buccal fat pad, lateral to the masseter muscle, before entering the buccal muscle. It is visible on T1W as a hypointense and on T2W images as a canalicular structure a few millimeters in diameter. Although the extraparotid segments of the duct can be followed, the intraparotid portions are not easily distinguishable. Similarly, it is difficult to determine the optimal course of the facial nerve within the parotid gland. Physiologically, numerous well-circumscribed, homogeneous cortical enhancement lymph nodes without necrosis can be observed within the gland. Lastly, the external carotid



**TABLE 6:** Diagnostic value of magnetic resonance imaging in predicting malignant parotid gland tumors.

| Study                          | TP | TN | FP | FN | Sensitivity (95% CI) | Specificity (95% CI) |
|--------------------------------|----|----|----|----|----------------------|----------------------|
| Lechner et al. <sup>20</sup>   | 13 | 41 | 3  | 3  | 81                   | 93                   |
| Yerli et al. <sup>21</sup>     | 4  | 19 | 0  | 1  | 80                   | 100                  |
| Inohara et al. <sup>22</sup>   | 17 | 55 | 5  | 4  | 81                   | 92                   |
| Takashima et al. <sup>23</sup> | 13 | 30 | 22 | 7  | 65                   | 58                   |

TP: True positive; TN: True negative; FP: False positive; FN: False negative; CI: Confidence interval.

artery and retromandibular vein are visible as tubular structures with variable intensity on T1 images and a hyperintense appearance following gadolinium injection.<sup>17,18</sup>

Determining the origin of a tumor within the parotid gland is crucial for selecting the appropriate surgical approach, especially when the tumor is large or situated deep. Three criteria on MRI are instrumental in confirming the parotid origin of the lesion: Medial displacement of the parapharyngeal fat, the lateral center of mass relative to the parapharyngeal space, increased spacing between the posterior styloid process, and the anterior mandibular angle.<sup>11,19</sup>

In the literature, studies have investigated the diagnostic value of conventional MRI but have primarily focused on distinguishing between malignant or benign lesions, revealing sensitivity of 65-81% and specificity of 58-100% (Table 6).<sup>20-23</sup> Our result for the overall diagnostic capability of conventional MRI correlated with previous research with a sensitivity of 71.4% and specificity of 92%, mostly adhering with the results of Inohara and Lechner.<sup>20,22</sup>

We classified the lesions into four groups and then investigated the diagnostic values of MRI for these specific tumor groups. The results indicate that MRI effectively excludes suspected diagnoses, as shown by the high specificity and negative predictive value for overall and all tumor classifications. However, when examining the sensitivity and PPV, the strength of MRI decreased, especially for NCT. The sensitivity and PPV of MRI tend to increase in specific tumor groups such as PA and CAL.

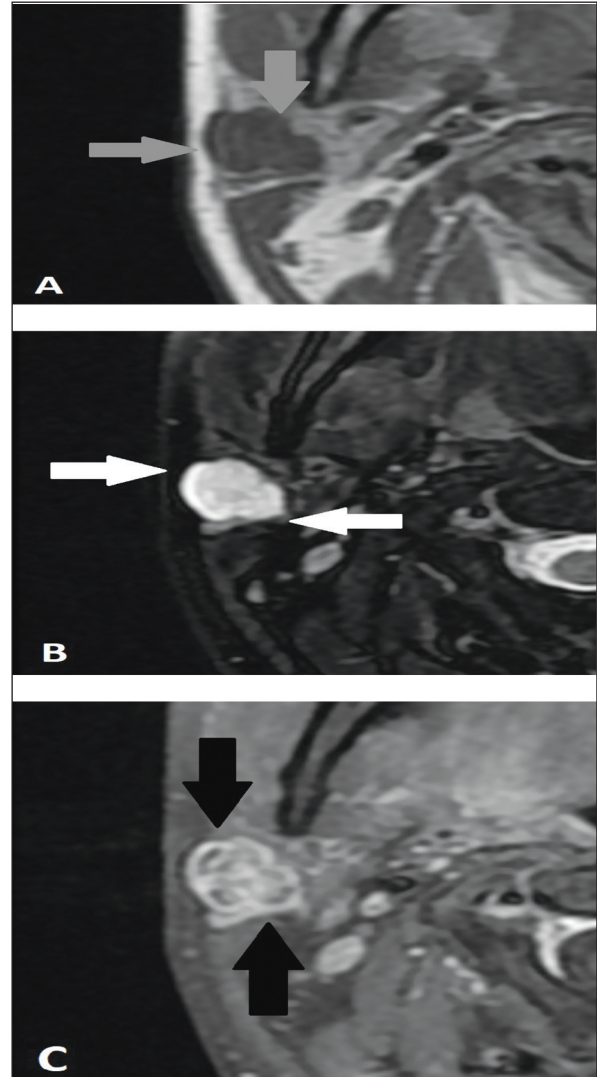


**FIGURE 2:** Presentation of pleomorphic adenoma in magnetic resonance imaging. **A)** Axial T1W image representing the hypointense tumor with lobulated margin (grey arrows); **B)** Axial T2W image illustrating the tumor with bright signal intensity and well demarcation line (white arrows); **C)** Axial T1W C+ with gadolinium scan shows heterogeneous contrast enhancement of the tumor (black arrows).

PA is the most common benign tumor found in the parotid gland. Macroscopically, it is well-demar-

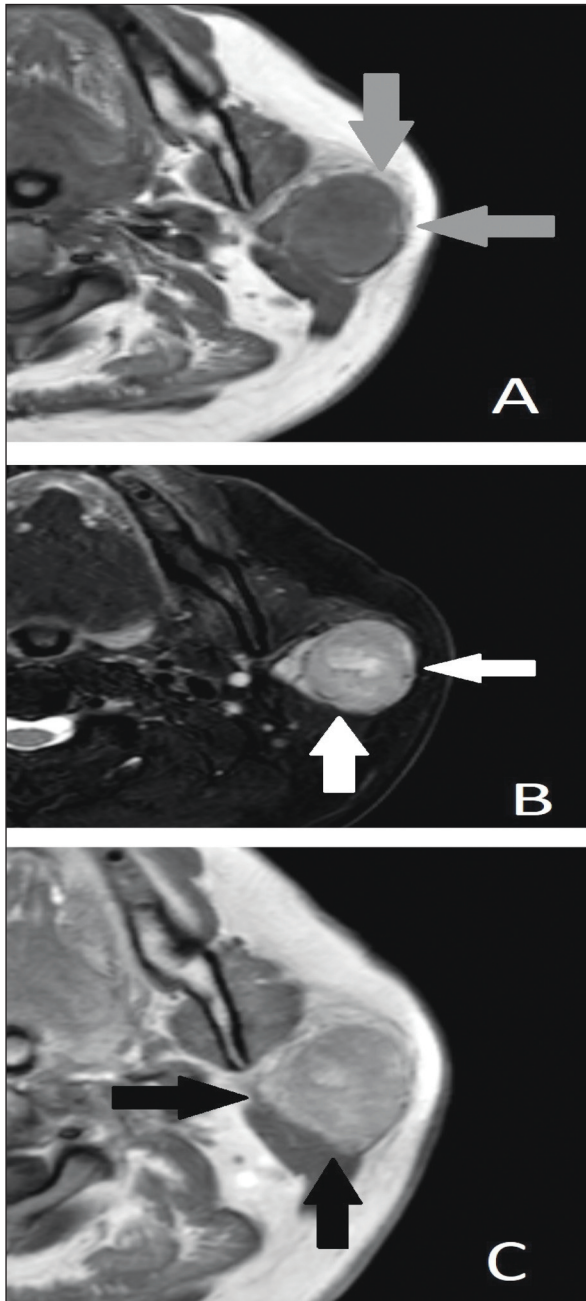


**FIGURE 3:** Presentation of cystadenoma lymphomatosum in magnetic resonance imaging. **A)** Axial T1W image showing a hypointense lesion with regular margins (grey arrows); **B)** Axial T2W image presenting the mass with moderate signal intensity (white arrows); **C)** Axial T1W C+ scan reveals moderate and heterogeneous enhancement with gadolinium (black arrows).

cated from the surrounding parenchymal tissue, has a lobulated contour, and may even include peripheral satellite nodules. Microscopically, it consists of a fibromyxoid stroma of the canalicular epithelium and spindle-shaped myoepithelial cells, which can vary

in appearance from myxoid, loose, or chondroid depending on their cell component. The characteristic hyperintense appearance on the T2W images is due to the water-rich nature of the myxoid component. Hypointense areas on T2W images can occur due to high cellularity.<sup>24</sup> Although the tumor is generally homogeneous, it can appear heterogeneous due to necrotic areas (Figure 2).<sup>25</sup>

Cystadenoma lymphomatosum, also known as Warthin's tumor, is the second most common benign tumor of the parotid gland, accounting for nearly 10% of cases.<sup>4</sup> Its soft consistency, well-defined boundaries, and cystic content characterize it. In approximately 10% of cases, the tumor can be multifocal or bilateral within the same gland.<sup>26</sup> Histologically, it includes cysts and pseudopapillary structures surrounded by large eosinophilic epithelial cells with an oncocytic appearance. A peripheral sheet of lymphoid tissue is typically observed. On MRI, CAL generally appears iso- or hypointense on T1W images, although rare nonspecific focal hyperintensities can be seen; on T2W images, it is typically hypo- or isointense. Gadolinium-enhanced imaging does not show enhancement (Figure 3).<sup>27</sup>

## CONCLUSION

This study highlights the significance of MRI in the diagnosis of parotid masses. It competes with FNAC, which performs cellular analysis regarding overall sensitivity, proving to be a successful non-invasive method. The specificity and negative predictive value were generally higher for all tumor classifications in the parotid gland. With identifiable specific MRI findings, the sensitivity and PPV increased for PA and Warthin's tumor. Considering the significance of not neglecting false positive and false negative cases, especially in NCT where the sensitivity of MRI significantly decreases, the combined use of MRI and FNAC still assists otolaryngology surgeons in managing parotid masses.

## Source of Finance

*During this study, no financial or spiritual support was received neither from any pharmaceutical company that has a direct con-*

nection with the research subject, nor from a company that provides or produces medical instruments and materials which may negatively affect the evaluation process of this study.

### Conflict of Interest

No conflicts of interest between the authors and / or family members of the scientific and medical committee members or members of the potential conflicts of interest, counseling, expertise, working conditions, share holding and similar situations in any firm.

### Authorship Contributions

**Idea/Concept:** Utku Mete, Rifat Özpar, Oğuz Basut; **Design:** Utku Mete, Rifat Özpar, Oğuz Basut; **Control/Supervision:** Özlem Saraydaroğlu, Oğuz Basut; **Data Collection and/or Processing:** Utku Mete, Rifat Özpar, Özlem Saraydaroğlu; **Analysis and/or Interpretation:** Utku Mete, Rifat Özpar, Oğuz Basut; **Literature Review:** Utku Mete, Rifat Özpar; **Writing the Article:** Utku Mete; **Critical Review:** Oğuz Basut; **References and Fundings:** Utku Mete, Rifat Özpar, Özlem Saraydaroğlu, Oğuz Basut; **Materials:** Utku Mete, Rifat Özpar, Özlem Saraydaroğlu, Oğuz Basut.

## REFERENCES

- Bishop JA, Thompson LDR, Wakely PE, Weinreb I. Tumors of the Salivary Glands. 1st ed. ARP Press; 2021. [Crossref]
- Skálová A, Hycza MD, Leivo I. Update from the 5th Edition of the World Health Organization Classification of Head and Neck Tumors: Salivary Glands. *Head Neck Pathol.* 2022;16(1):40-53. [Crossref] [PubMed] [PMC]
- Inaka Y, Kawata R, Haginomori SI, Terada T, Higashino M, Omura S, et al. Symptoms and signs of parotid tumors and their value for diagnosis and prognosis: a 20-year review at a single institution. *Int J Clin Oncol.* 2021;26(7): 1170-8. [Crossref] [PubMed]
- Silvers AR, Som PM. Salivary glands. *Radiol Clin North Am.* 1998;36(5):941-66, vi. [Crossref] [PubMed]
- Batsakis JG. Tumors of the Head and Neck. 2nd ed. Baltimore: Williams & Wilkins; 1979. [Crossref] [PubMed]
- Ginat DT. Imaging of benign neoplastic and nonneoplastic salivary gland tumors. *Neuroimaging Clin N Am.* 2018;28(2):159-69. [Crossref] [PubMed]
- Ozawa N, Okamura T, Koyama K, Nakayama K, Kawabe J, Shiomi S, et al. Retrospective review: usefulness of a number of imaging modalities including CT, MRI, technetium-99m pertechnetate scintigraphy, gallium-67 scintigraphy and F-18-FDG PET in the differentiation of benign from malignant parotid masses. *Radiat Med.* 2006;24(1):41-9. [Crossref] [PubMed]
- Rabinov JD. Imaging of salivary gland pathology. *Radiol Clin North Am.* 2000;38(5):1047-57, x-xi. [Crossref] [PubMed]
- Shah GV. MR imaging of salivary glands. *Neuroimaging Clin N Am.* 2004;14(4):777-808. [Crossref] [PubMed]
- Christe A, Waldherr C, Hallett R, Zbaeren P, Thoeny H. MR imaging of parotid tumors: typical lesion characteristics in MR imaging improve discrimination between benign and malignant disease. *AJNR Am J Neuro-radiol.* 2011;32(7):1202-7. [Crossref] [PubMed] [PMC]
- Goto TK, Yoshiura K, Nakayama E, Yuasa K, Tabata O, Nakano T, et al. The combined use of US and MR imaging for the diagnosis of masses in the parotid region. *Acta Radiol.* 2001;42(1):88-95. [Crossref] [PubMed]
- Paris J, Facon F, Pascal T, Chrestian MA, Moulin G, Zanaret M. Preoperative diagnostic values of fine-needle cytology and MRI in parotid gland tumors. *Eur Arch Otorhinolaryngol.* 2005;262(1):27-31. [Crossref] [PubMed]
- Casselmann JW, Mancuso AA. Major salivary gland masses: comparison of MR imaging and CT. *Radiology.* 1987;165(1):183-9. [Crossref] [PubMed]
- Teresi LM, Lufkin RB, Wortham DG, Abemayor E, Hanafee WN. Parotid masses: MR imaging. *Radiology.* 1987;163(2):405-9. [Crossref] [PubMed]
- Heiss R, Nagel AM, Laun FB, Uder M, Bickelhaupt S. Low-field magnetic resonance imaging: a new generation of breakthrough technology in clinical imaging. *Invest Radiol.* 2021;56(11):726-33. [Crossref] [PubMed]
- Suzuki H, Takeuchi Y, Numata T, Tsukuda T, Shimada F, Konno A, et al. [Ultrasonographic diagnosis of the parotid gland tumors—experience with 310 patients]. *Nihon Jibiinkoka Gakkai Kaiho.* 1997;100(9):893-9. Japanese. [Crossref] [PubMed]
- Prasad RS. Parotid gland imaging. *Otolaryngol Clin North Am.* 2016;49(2):285-312. [Crossref] [PubMed]
- Kanekar SG, Mannion K, Zacharia T, Showalter M. Parotid space: anatomic imaging. *Otolaryngol Clin North Am.* 2012;45(6):1253-72. [Crossref] [PubMed]
- Joe VQ, Westesson PL. Tumors of the parotid gland: MR imaging characteristics of various histologic types. *AJR Am J Roentgenol.* 1994;163(2):433-8. [Crossref] [PubMed]
- Lechner Goyault J, Riehm S, Neuville A, Gentine A, Veillon F. Interest of diffusion-weighted and gadolinium-enhanced dynamic MR sequences for the diagnosis of parotid gland tumors. *J Neuroradiol.* 2011;38(2):77-89. [Crossref] [PubMed]
- Yerli H, Aydin E, Haberal N, Harman A, Kaskati T, Alibek S. Diagnosing common parotid tumours with magnetic resonance imaging including diffusion-weighted imaging vs fine-needle aspiration cytology: a comparative study. *Dentomaxillofac Radiol.* 2010;39(6):349-55. [Crossref] [PubMed] [PMC]
- Inohara H, Akahani S, Yamamoto Y, Hattori K, Tomiyama Y, Tomita Y, et al. The role of fine-needle aspiration cytology and magnetic resonance imaging in the management of parotid mass lesions. *Acta Otolaryngol.* 2008;128(10):1152-8. [Crossref] [PubMed]



23. Takashima S, Wang J, Takayama F, Momose M, Matsushita T, Kawakami S, et al. Parotid masses: prediction of malignancy using magnetization transfer and MR imaging findings. *AJR Am J Roentgenol.* 2001;176(6):1577-84. [[Crossref](#)] [[PubMed](#)]
24. Tsushima Y, Matsumoto M, Endo K, Aihara T, Nakajima T. Characteristic bright signal of parotid pleomorphic adenomas on T2-weighted MR images with pathological correlation. *Clin Radiol.* 1994;49(7):485-9. [[Crossref](#)] [[PubMed](#)]
25. Okahara M, Kiyosue H, Hori Y, Matsumoto A, Mori H, Yokoyama S. Parotid tumors: MR imaging with pathological correlation. *Eur Radiol.* 2003;13 Suppl 4:L25-33. [[Crossref](#)] [[PubMed](#)]
26. Lin CC, Tsai MH, Huang CC, Hua CH, Tseng HC, Huang ST. Parotid tumors: a 10-year experience. *Am J Otolaryngol.* 2008;29(2):94-100. [[Crossref](#)] [[PubMed](#)]
27. Minami M, Tanioka H, Oyama K, Itai Y, Eguchi M, Yoshikawa K, et al. Warthin tumor of the parotid gland: MR-pathologic correlation. *AJNR Am J Neuroradiol.* 1993;14(1):209-14. [[PubMed](#)] [[PMC](#)]